POLISH POLAR RESEARCH
vol. 32, no. 1, pp. 39–58, 2011 doi: 10.2478/v10183-011-0006-8

Cenozoic stress field in the southwestern Antarctic Peninsula from brittle mesostructures in Wright Peninsula, Adelaide Island

Adolfo MAESTRO [1,2]* and Jerónimo LÓPEZ-MARTÍNEZ [2]

[1] *Instituto Geológico y Minero de España, Ríos Rosas, 23, 28003 Madrid, Spain*
*<a.maestro@igme.es> * corresponding author*

[2] *Departamento de Geología y Geoquímica, Facultad de Ciencias, Universidad Autónoma de Madrid, 28049 Madrid, Spain*
<jeronimo.lopez@uam.es>

Abstract: Palaeostresses inferred from brittle mesostructures in the southern Wright Peninsula show a stress field characterized by compressional, strike-slip and extensional regime stress states. The compressional stress (σ_1) shows a main NW-SE direction and the extensional stress (σ_3) shows a relative scattering with two main modes: NE-SW to E-W and NW-SE. The maximum horizontal stress (σ_y) has a bimodal distribution with NW-SE and NE-SW direction. The compressional orientation is related to subduction of the former Phoenix Plate under the Antarctic Plate from the Early Jurassic to the Early Miocene. Extensional structures within a broad-scale compressional stress field can be related to both the decrease in relative stress magnitudes from active margins to intraplate regions and stretching processes occurring in eastern Adelaide Island, which develop a fore-arc or intra-arc basin from the Early Miocene. Stress states with NW-SE-trending σ_1 are compatible with the dominant pattern established for the western Antarctic Peninsula. NW-SE orientations of σ_3 suggest the occurrence of tectonic forces coming from fore-arc extension along the western Antarctic Peninsula.

Key words: Antarctica, Adelaide Island, fore-arc basin, palaeostress orientation.

Introduction

Cenozoic tectonic stress in the southwestern part of the Antarctic Peninsula is not well defined due primarily to scarcity of outcropping rock and a lack of recorded seismicity. However, tectonic stress studies in this area are interesting for developing a better understanding of the net effects of plate-boundary processes. The western sector of the Antarctic Peninsula represents a long-lived, continental margin magmatic arc produced in response to subduction of oceanic lithosphere at

a trench formerly situated off the western coast (Suárez 1976; Fig. 1A). Subduction is known to have been active mainly between Early Jurassic and Miocene times (Pankhurst 1982).

In this paper we present palaeostress indicators obtained from fault, joint and basaltic dyke population analysis in early Paleocene–Eocene igneous rocks of the southern Wright Peninsula. The mentioned area is located in the central-eastern part of Adelaide Island (Fig. 1B). This island is bounded to the west by a shelf-break towards the oceanic crust of the Pacific Ocean and to the east, through steep faults, by the Antarctic Peninsula. In the context of contributing to knowledge of the tectonic evolution of the western margin of the Antarctic Peninsula, the main objectives of this work are: (i) to characterize the Cenozoic compressional and extensional stress field in the southwestern part of the Antarctic Peninsula and (ii) to determine the stress evolution that may have been responsible for the orientation of the stress fields acting in this area during the Cenozoic.

Geological setting

During most of the Mesozoic and Cenozoic the Antarctic Peninsula was an active volcanic arc, resulting from eastward-dipping subduction of oceanic crust of the former Phoenix Plate beneath the continental crust of the Antarctic Peninsula (Pankhurst 1982; Storey and Garret 1985). The subduction ceased progressively northward due to the arrival of segments of the Antarctic-Phoenix ridge at the subduction trench (Herron and Tucholke 1976), resulting in the formation of a passive margin at the boundary between the trailing flank of the ridge and the Peninsula, both of which formed part of the Antarctic Plate (Barker 1982; Larter and Barker 1991). Arrival dates of the ridge segments along the western flank of the Antarctic Peninsula were calculated by Larter *et al.* (1997), using the geomagnetic polarity time scale of Cande and Kent (1995). The earliest collisions took place off Ellsworth Land and southern Alexander Island, between ~63 and 45 Ma. Subsequent ridge crest-trench collisions caused subduction to cease at 19.8±0.8 Ma off Marguerite Bay, 16.5±0.7 Ma off Adelaide Island and the southern Biscoe Islands, and 14.5±0.6 Ma off the northern Biscoe Islands. The Phoenix Plate became part of the Antarctic Plate when sea-floor spreading stopped in the Drake Passage 3.3 Ma ago, an event interpreted to have shut down subduction at the South Shetland Trench thrust (Livermore *et al.* 2000; Eagles 2003).

Pre-Mesozoic basement gneiss and orthogneiss is exposed in eastern Graham Land (Milne and Millar 1989) and in northwest Palmer Land (Harrison and Piercy 1991). Calc-alkaline volcanic and plutonic rocks crop out long the length of the peninsula (Pankhurst 1982). The plutonic rocks form the Antarctic Peninsula Batholith (Leat *et al.* 1995). Volcanic rocks of the Antarctic Peninsula Volcanic Group are genetically related to the plutonic rocks of northern Palmer Land (Leat and Scarrow

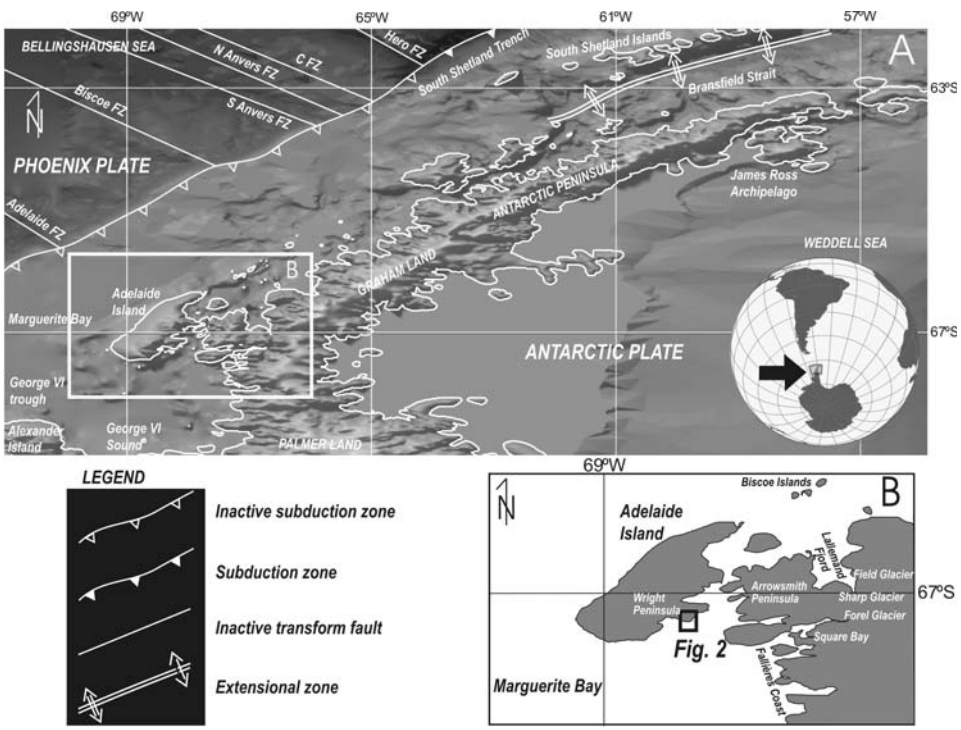

Fig. 1. **A**. Regional tectonic framework and digital terrain model map of the northern Antarctic Peninsula region. Topographic and bathymetric map derived from satellite and ship track data (Smith and Sandwell 1997). Southern Wright Peninsula in Adelaide Island is marked by a box. **B**. Main geographical features around Adelaide Island.

1994). Magmatism reached a peak in early Cretaceous times, with intrusions of this age dated in all parts of the peninsula (145.6–97 Ma; Leat *et al.* 1995). Cenozoic arc-related magmatism appears to have been limited to the western side of the peninsula, which suggests a westward migration of the arc (Pankhurst 1982).

On Adelaide Island, located on the western seaboard of the Antarctic Peninsula, a 2.5 km thick sedimentary and volcanic succession of late Mesozoic to early Cenozoic age belonging to the Antarctic Peninsula Volcanic Group is exposed (Thomson 1982; Moyes *et al*. 1994). The island is situated on the western flank of the arc, in a fore-arc or intra-arc position. In the Early Tertiary, westward migration of the arc towards the ocean trench was associated with plutonism on Adelaide Island (Pankhurst 1982; Pankhurst *et al*. 1988) and was part of the Antarctic Peninsula Batholith (Leat *et al*. 1995). In the 1980s a small number of volcanic and plutonic rocks from Adelaide Island and its vicinity were dated by Rb-Sr methods. A rhyolite from Webb Island has a poorly constrained age of 67±17 Ma (Thomson and Pankhurst 1983; Moyes *et al.* 1994). Granodiorite-granite plutons; on Wright Peninsula and Anchorage Island have Early Tertiary ages of 60±3 and 62±2 Ma, respectively (Pankhurst 1982; see Fig. 2). Finally, Griffiths and Oglethorpe (1998)

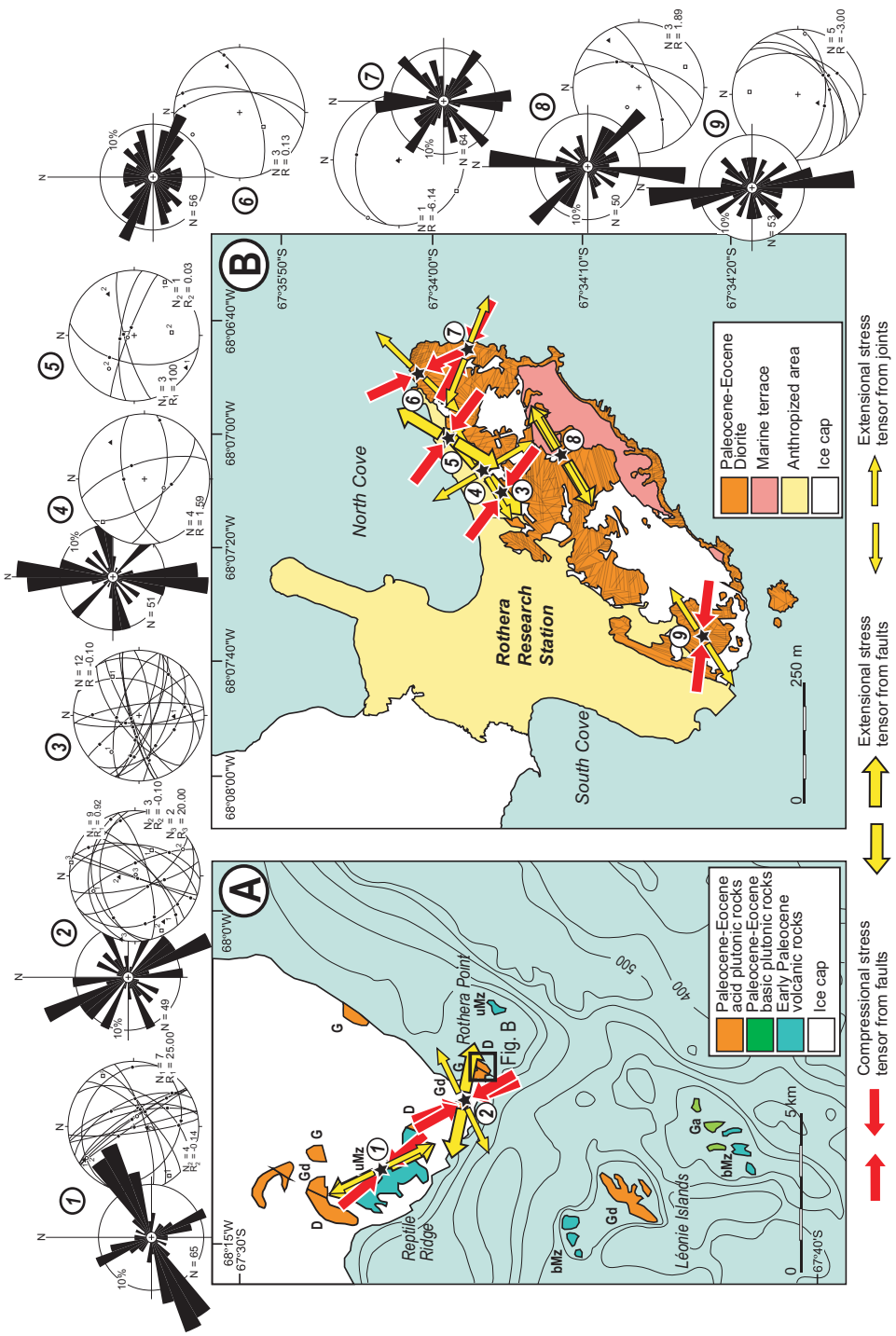
A
B
68°15'W
67°30'S
68°0'W
67°40'S
Reptile Ridge
Rothera Point
Fig. B
Léonie Islands
North Cove
South Cove
Rothera Research Station
68°8'00"W
68°0'40"W
68°7'20"W
68°7'00"W
68°6'40"W
67°35'50"S
67°34'00"S
67°34'10"S
67°34'20"S
0
250 m
5 km
Paleocene-Eocene acid plutonic rocks
Paleocene-Eocene basic plutonic rocks
Early Paleocene volcanic rocks
Ice cap
Paleocene-Eocene Diorite
Marine terrace
Anthropized area
Ice cap
Compressional stress tensor from faults
Extensional stress tensor from faults
Extensional stress tensor from joints

used multiple methods of dating (^{40}Ar-^{39}Ar, K-Ar, fission track) in order to constrain the stratigraphy of Adelaide Island, to show how sedimentation and volcanism changed with time and, where possible, to correlate these changes with known large-scale tectonic developments in the Antarctic Peninsula.

Palaeostress analysis of brittle mesostructures

The analysis of data has been made by using a sequence of three methods, each one providing a different approach to the stress determination problem, whose joint usefulness has been broadly tested in the past years (Casas *et al.* 1992; Casas and Maestro 1996) and enables the complete definition of stress tensors (Fig. 3):

(a) Right Dihedra method (Angelier and Mechler 1977). This is a simple geometrical approach which provides an initial estimate of stress directions.

(b) y-R diagram (Simón 1986). It is a 2D approximation in which one of the principal stress axes is supposed to be vertical, so that tensors may be represented only by two parameters: y (azimuth of the maximum horizontal stress, σ_y) and R (stress ratio in Bott's equation, $R = (\sigma_z - \sigma_x)/(\sigma_y - \sigma_x)$). The y, R pairs satisfying one individual fault give rise to a curve; the 'knots' where these curves intersect show a preliminary spectrum of all possible solutions and their relative weight in the whole fault population (especially useful in the case of polyphase tectonics or when a gradual tensor change occurs). The knots of y-R diagram have to be corroborated by other three-dimensional method (*e.g.* Etchecopar's method) and they we can conclude that the solutions determined represent true stress tensors showing a vertical axis (σ_1, σ_2 or σ_3, according to R value).

(c) Etchecopar's method (Etchecopar *et al.* 1981). This is a numerical method which allows the exploration of the solutions suggested by the y-R and Right Dihedra diagrams. These solutions will eventually be confirmed and refined in order to obtain the final, complete solution: 3D orientations of the three principal stress axes and stress ratio. Etchecopar's method is based upon the minimization of the angles between real and theoretical striations, it allows the separation of different stress tensors by means of an adequate management of the percentage of data submitted to minimization. After this preliminary analysis, we chose the solution that explained most faults with a good histogram of angular discrepancies and a good distribution of explained faults on the Mohr circle. In monophase popula-

← Fig. 2. **A**. Geological sketch map of the southern Wright Peninsula (modified from Moyes *et al.* 1994) and location of study sites. D, diorite; G, granite; Ga, gabbro; Gd, granodiorite; bMz, basic to intermediate volcanic rocks; uMz, undifferentiated volcanic rocks. **B**. Geological sketch map of Rothera Point and location of study sites. Stereoplots include fault planes and slickenside striations, stress axes (σ_1, white circle; σ_2, white square; and σ_3, black triangle). Rose diagrams of orientation of joints (black roses) on the outcrop scale (outer circle represents 10% of the data set in the site); R, stress ratio; N, number of data.

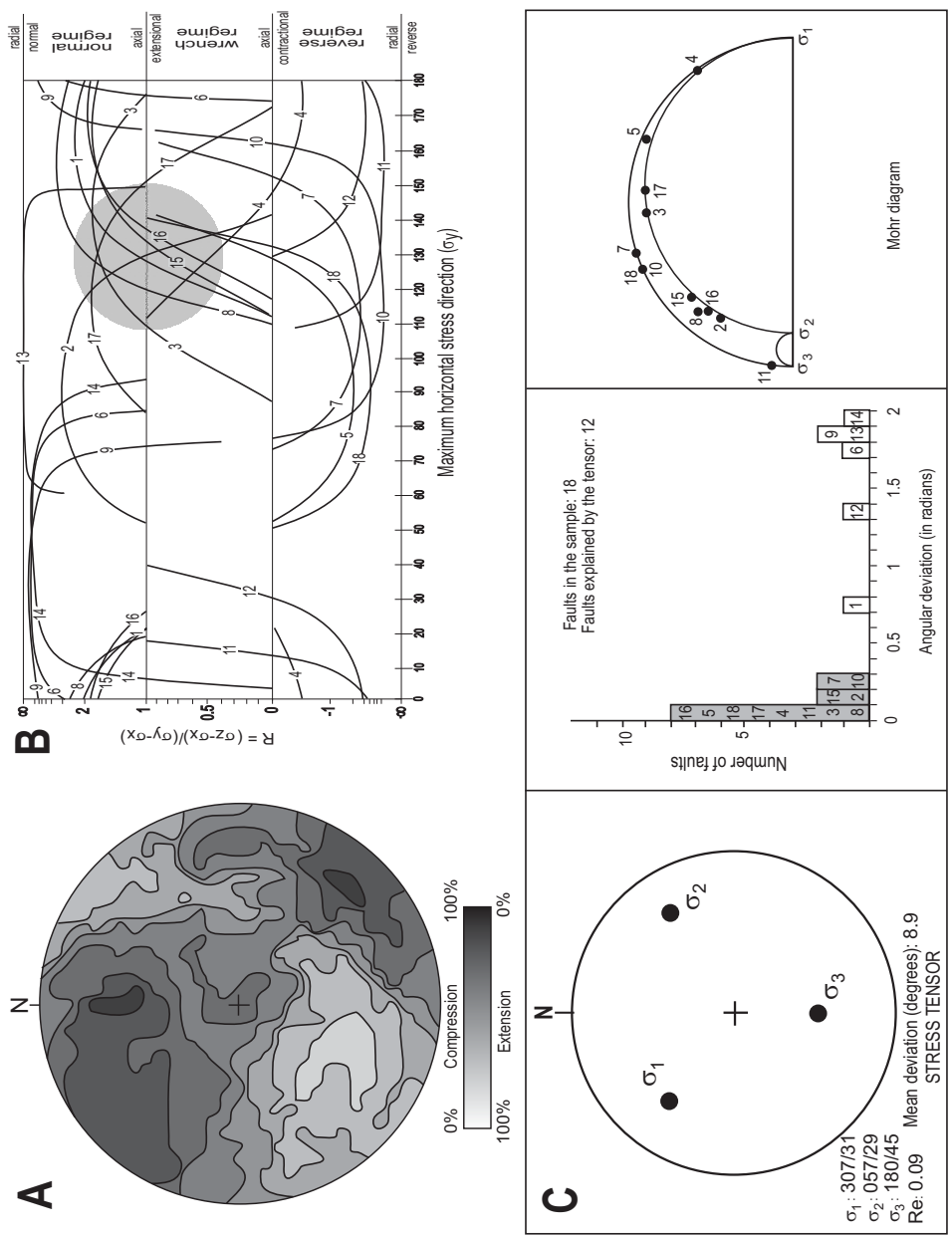

Fig. 3. Example of standard stress analysis of a fault population (station 3). See location on map and equal-area plot of fault data in Fig. 2. **A**. Right Dihedra diagram (Schmidt net, lower hemisphere); isolines express the percentage of faults compatible with an extension axis. **B**. y-R diagram; y is the azimuth of the maximum horizontal stress σ_y; $R = (\sigma_z - \sigma_x)/(\sigma_y - \sigma_x)$; the shaded ellipses indicate the zones showing the highest density of curve intersections, and so the optimum stress tensors. **C**. Results of Etchecopar's method: stereoplot of the inferred stress axes, $R_e = (\sigma_2 - \sigma_3)/(\sigma_1 - \sigma_3)$; histogram of angular deviations between actual striation and theoretical shear component on each fault; Mohr diagram where the planes corresponding to the explained faults are plotted.

tions a satisfactory solution is normally obtained for 80–90% of faults, thus rejecting 10–20% of spurious data. In suspected polyphase populations the initial required percentage should be lower (30–50%); the program chooses the best fitting faults representing this initial percentage, which are then discarded in order to find a second stress solution. Reliability of calculated solutions can be tested using random sub-sampling analysis (Arlegui and Simón 1998). Occurrence of different stress tensors with similar orientations at the same site could be related to local perturbations of the regional stress field.

In addition to faults, joints have also been used to establish palaeostress fields during the Cenozoic. Joints in granitic rock masses can be caused by a combination of extrinsic stresses (*e.g.* remote tectonic stresses, stresses related to nearby pluton emplacement, or stresses associated with erosion of the overburden) and intrinsic stresses (*e.g.* pore fluid pressures, thermal stresses associated with pluton cooling). In many cases it is difficult to differentiate joints caused for extrinsic or intrinsic stresses in igneous rocks. The origin is clear in cases like joint exfoliations related to unload-decompression processes in plutonic rocks, or columnar joints in volcanic rocks developed during the cooling processes. Other joints related to the cooling processes of magmatic masses can be identified by their random orientations and not considered in the tectonic interpretation. In this study, the joint population data have been processed by statistical methods that allowed establishing the preferential strikes affecting the volcanic and plutonic rocks outcropping in the area. 439 joints have been measure in eight different sites (Fig. 2). In all of them the number of data is enough to characterizing the reliable fracture pattern at each site according with Arlegui and Simón (2001).

Several studies focus on the mechanical interpretation of joints as regional stress indicators (*e.g.* Engelder and Geiser 1980; Hancock and Engelder 1989, among others). Many authors consider the existence of tension and shear joints (*e.g.* Hanckock, 1985) which provides a very accurate interpretation of the maximum horizontal (σ_y) and extensional (σ_3) stress trends, although no quantitative estimation of the stress ratio can be made. Other authors assume that every joint is a mode I fracture normal to σ_3 (*e.g.* Engelder and Geiser 1980, Pollard and Aydin 1988). However, this assumption cannot be considered due to the abundant field evidences demonstrating the existence of shear and hybrid/shear tension joints: (1) synchronous joints arranged in conjugate pairs showing low dihedral angles (Hancock 1985; Bergerat *et al.* 1992), (2) joints oblique to σ_1 and σ_3 axes independently determined from different structures (Bergerat *et al.* 1992), (3) joint spectra, as defined by Hanckock (1986) (Arlegui and Simón 1998), and (4) kinematic indicators on joint surfaces. Quite often, joints arranged in low-dihedral conjugate pairs display en èchelon microfractures randomly located within the parent joints. As they are not confined to the fringe zone, they cannot be interpreted as f joints (Hodgson 1961) related to fracture propagation and plume formation (Bahat 1991). On the contrary, they are shear Riedel fractures (Riedel 1929) which may be used as shear indicators (Engelder

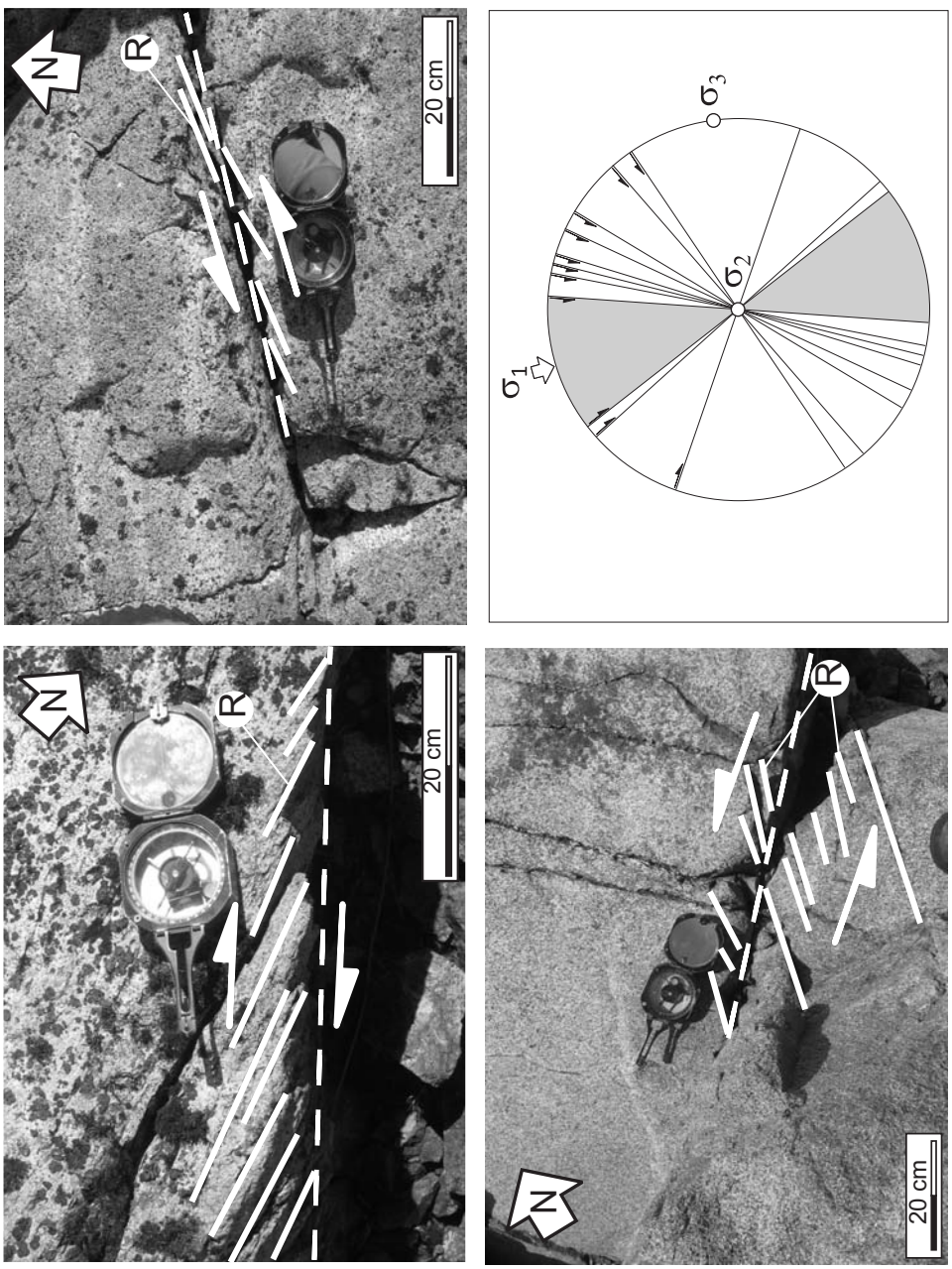

Fig. 4. Examples of shear (left lateral and right lateral) joints showing en èchelon Riedel minor fractures (R) with no observed offset. Stereogram with the orientation of conjugate shear planes measured in the study are compatible with a horizontal NW-SE trending σ_1 axis.

1989; Arlegui and Simón 2001; Simón *et al.* 2006). In this study several joint planes showing shear Riedel fractures have been observed (Fig. 4).

Cenozoic stress field

Palaeostress analysis was performed using brittle mesostructures, mainly striated fault planes and tension and shear joints, measured at 9 sites in Early Paleocene–Eocene igneous rocks (Fig. 2). Sixty-seven striated faults (9 sites), around 400 extension and shear joints (7 sites) and four basaltic dykes (1 site) were measured in the field and analyzed. Small-offset normal faults (approximately 40) dominate on the scale of exposure, although 17 reverse faults and 9 left-lateral and 5 right-lateral strike-slip faults were recognized. In both cases, slip on the majority of fault planes varies from centimeters to a few meters. Most joint planes are vertical, whereas normal and reverse faults dip between 20° and 80°. Overall, fractures on the outcrop scale show NNW-SSE to N-S, ENE-WSW and ESE-WNW orientation maxima. Directional analysis of faults also reveals three relative maxima striking NNE-ESE, NE-SW and NW-SE. Joint data show a relative maximum striking N-S and two relative maxima striking NE-SW and NW-SE.

Regional morphostructural features are widespread in the southern Antarctic Peninsula (*e.g.* Moyes *et al.* 1994), and are mainly identified from physiographic rather than clear geological evidence. The dominant on-shore geomorphological feature in this area is a N-NNE trending depression, which extends northward from Square Bay to Field Glacier, inland from Fallières Coast, between the Forel and Sharp glaciers. This depression separates two distinct areas – Adelaide Island and the western coast of the Antarctic Peninsula – from the plateau and eastern coastal regions of the Peninsula. In the western area the N-NNE trend is also reflected in dyke orientations and joint surfaces, and a further expression of it can be observed in the orientation of the Lallemand Fjord trough. The NE trend of the major features in this area (particularly on Adelaide Island and in northern Marguerite Bay) in addition to some dykes that also follow a NE trend, suggest the existence of a second set of lineaments. A third, but less prominent set of lineaments with a NNW trend is emphasized by the orientation of several large glaciers, and by a number of dykes and joint surfaces observed on Adelaide Island and Arrowsmith Peninsula. To the east of the topographic depression between the Forel and Sharp glaciers a number of E- or ENE-trending features, such as glaciers, can be correlated with observed faulting on the east coast, with the majority of dyke orientations and with joint surfaces recorded on plutonic rocks. A N- or NW-trending set of lineaments is also apparent in this region, reflected mainly in the orientation of a few dykes and joint surfaces on outcrops of volcanic rocks. Johnson (1997) mapped lineaments and trends using the magnetic anomaly, bathymetry, free-air gravity and Bouguer gravity maps. The shelf edge and mid shelf high anomalies trend NE-SW across the western part of Adelaide Island, and several trends parallel to this closer to the Antarctic Peninsula. The predominant trend directions in Marguerite Bay are NW-SE. The trend of George VI Sound and George VI trough is NNW-SSE.

Table 1

Summary of stress tensors and stress orientations obtained from brittle mesostructure population analysis. Sites are located in Fig. 2; age of rock, plutonic and volcanic rock classification according to Streckeisen (1976); σ_1, σ_2 and σ_3, values of principal stress axes; σ_y, maximum horizontal stress; Re, stress ratio = $(\sigma_2 - \sigma_3)/(\sigma_1 - \sigma_3)$ (Etchecopar *et al.* 1981); Rb, stress ratio = $(\sigma_z - \sigma_x)/(\sigma_y - \sigma_x)$ (Bott 1959). Structures: ND, number of data measured at each site; n/N, number of data used for defining each stress state/number of faults in the fault population.

Site	Age of rocks	Rocks	σ_1	σ_2	σ_3	σ_y	Re	Rb	Structure	ND	n/N
1	Early Paleocene	Rhyolite	110/76	234/08	326/11	234/08	0.04	25.00	Faults	15	7/15
1	Early Paleocene	Rhyolite	326/15	059/10	181/72	326/15	0.12	-0.14	Faults	15	4/15
1	Early Paleocene	Rhyolite	–	–	155/00	065/00	–	–	Joints	65	–
2	Paleocene–Eocene	Granodiorite	340/33	123/51	237/19	340/33	0.92	0.92	Faults	14	9/14
2	Paleocene–Eocene	Granodiorite	151/17	244/08	359/71	151/17	0.09	-0.10	Faults	14	3/14
2	Paleocene–Eocene	Granodiorite	121/88	012/01	282/02	012/01	0.05	20.00	Faults	14	2/14
2	Paleocene–Eocene	Granodiorite	–	–	065/00	155/00	–	–	Joints	49	–
3	Paleocene–Eocene	Diorite	307/31	056/29	180/45	307/31	0.09	-0.10	Faults	18	12/18
4	Paleocene–Eocene	Diorite	204/63	314/10	049/25	314/10	0.63	1.59	Faults	4	4/4
4	Paleocene–Eocene	Diorite	150/00	000/90	060/00	150/00	–	–	Joints	51	–
4	Paleocene–Eocene	Diorite	060/00	000/90	150/00	060/00	–	–	Joints	51	–
5	Paleocene–Eocene	Diorite	344/82	120/06	211/06	120/06	0.01	100.00	Faults	4	3/4
5	Paleocene–Eocene	Diorite	307/37	175/42	059/26	307/37	0.03	0.03	Faults	4	1/4
6	Paleocene–Eocene	Diorite	335/22	210/55	076/26	335/22	0.13	0.13	Faults	3	3/3
6	Paleocene–Eocene	Diorite	135/00	000/90	045/00	135/00	–	–	Joints	56	–
6	Paleocene–Eocene	Rhyolite	–	–	067/00	157/00	–	–	Dykes	4	–
7	Paleocene–Eocene	Diorite	298/00	208/00	53/90	298/00	0.86	-6.14	Faults	1	1/1
7	Paleocene–Eocene	Diorite	022/00	000/90	112/00	022/00	–	–	Joints	64	–
8	Paleocene–Eocene	Diorite	300/62	156/23	059/15	156/23	0.53	1.89	Faults	3	3/3
8	Paleocene–Eocene	Diorite	–	–	060/00	150/00	–	–	Joints	50	–
9	Paleocene–Eocene	Diorite	097/07	003/27	200/62	097/07	0.75	-3.00	Faults	5	5/5
9	Paleocene–Eocene	Diorite	148/00	000/90	058/00	148/00	–	–	Joints	53	–

The coincidence of a number of interpreted magnetic, gravity and bathymetric trends in the centre of Marguerite Bay suggest fault control (Johnson 1997).

The results of palaeostress analysis (by means of the three methods mentioned above) are summarized in Table 1. Stress tensors are included, giving σ_1, σ_2, σ_3 and σ_y orientations and the values of R and Re. The number of data used to define each stress state vs. number of faults in the fault population is also shown.

In order to present a graphical view of the stress tensor directions obtained in the southern Wright Peninsula, two kinds of representation were prepared: (1) the projection of the σ_1, σ_3 and σ_y axes of all the stress tensors obtained from fault slip

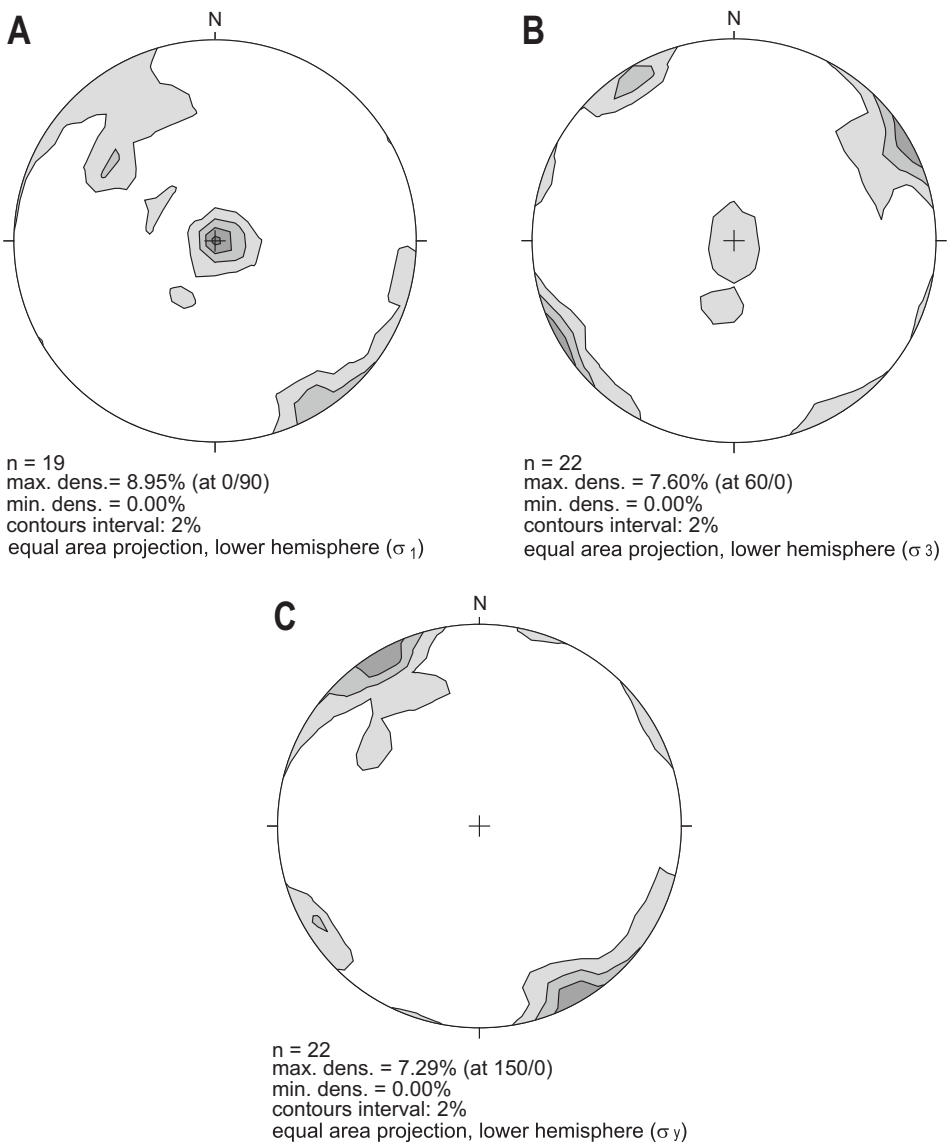

Fig. 5. Density stereoplots representing: A, compression (σ_1); B, extension (σ_3), and C, greatest horizontal stress (σ_y) axes obtained from analysis of brittle mesostructures. Equal area projection, lower hemisphere.

data sets by Etchecopar's method, joints and basaltic dykes, respectively (Fig. 5), and (2) the graphical representation of fault planes by means of the y-R diagram (Simón 1986), showing the orientation of the maximum horizontal stress axes and their associated stress regime (Fig. 6). The results obtained with the y-R method showed orientations of maximum horizontal shortening very similar to those inferred by Etchecopar's method.

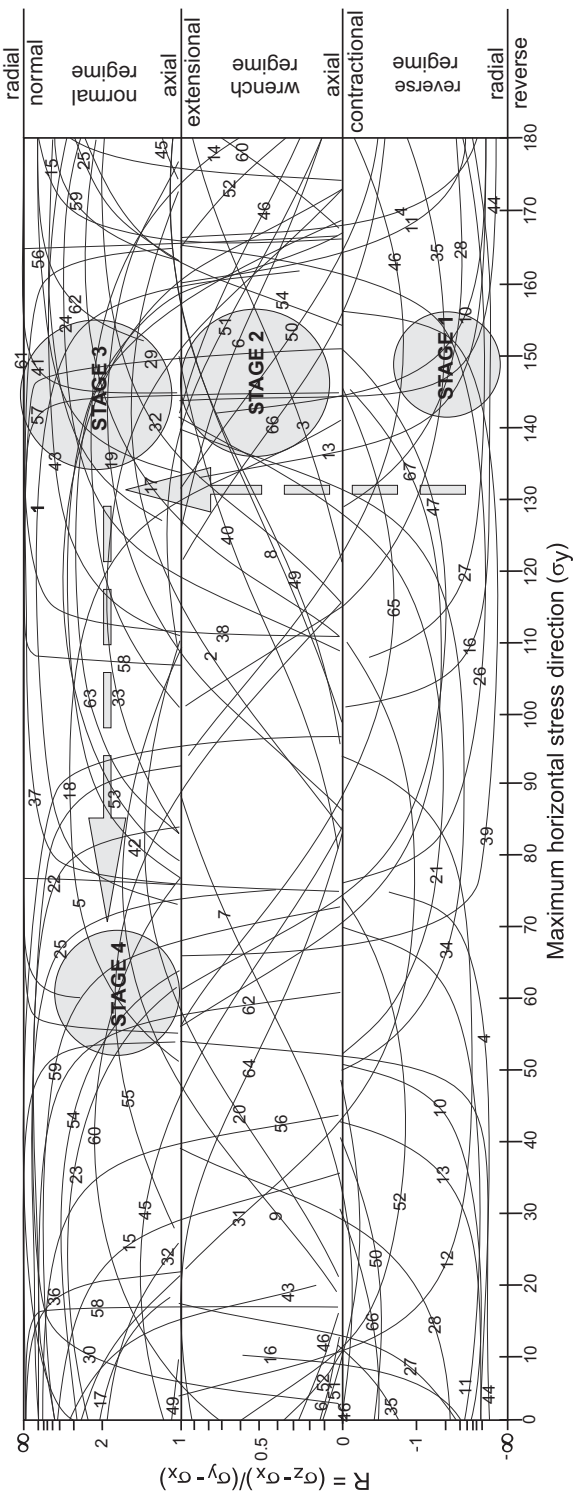

Fig. 6. y-R diagram of the fault planes measured in this work. σ_y is the azimuth of the major horizontal axis; $R = (\sigma_z - \sigma_x)/(\sigma_y - \sigma_x)$, where σ_z is vertical and $\sigma_y > \sigma_x$ (Bott 1959). The circles indicate the zones showing the highest density of curve intersections. To the right, stress regimes corresponding to the various values of the stress ellipsoid shape ratio are indicated.

From the orientations of stress axes it can be seen that there is a dominant NW-SE horizontal compression direction (Fig. 5A) and two NW-SE and NE-SW minor horizontal stress directions (Fig. 5B). Orientations of σ_y show two main modes trending NW-SE and NE-SW (Fig. 5C). The NW-SE maximum stress direction shows an R relationship ranging from reverse to normal regimes (Fig. 6). The NE-SW mode corresponds to extensional stress tensors (Fig. 6). The relative chronology between extensional and compressional structures is not clear. Furthermore, chronological relationships between NE-SW and NW-SE σ_3 orientations cannot be established since both directions were inferred from Early Paleocene–Eocene igneous rocks.

Discussion

There is no clear geodynamic model for explaining the several orientations of σ_y recorded from Early Paleocene–Eocene rocks in the southern Wright Peninsula. Similarly, relationships between local tectonic stresses and the broad-scale Antarctic Peninsula stress field during the Cenozoic are ambiguous.

The principal stress orientations are usually constant and parallel to the absolute plate motions (Zoback 1992). However, in many intraplate tectonic areas and at some plate tectonic boundaries, stress analysis of recent structures shows several contemporary stress tensors. These generally differ in the orientation of their principal stress axes. This has been interpreted as the consequence of active tectonic deformation processes occurring consecutively over a long period of time, but many of these stress tensor orientations are probably coeval. In intraplate areas, these different stress tensors have also been explained as the result of coetaneous stress fields transmitted from the active plate boundaries, which react among themselves to yield changes in the shape and orientation of the stress tensor (De Vicente *et al.* 1996; Herraiz *et al.* 2000). However, in some places, it has been demonstrated that similar changes or permutations in principal stress orientations have occurred repeatedly in space and time (Bergerat *et al.* 1999; García *et al.* 2002; Giner-Robles *et al.* 2003).

In the area studied in this work, two maximum horizontal shortening directions were found:

- A NW maximum horizontal shortening direction (σ_y) deduced from fault population analysis (Fig. 6). It was assumed that this stress tensor defines the convergent regime in this zone and therefore represents the primary stress tensor of the whole area.
- A NE orientation of maximum horizontal shortening (σ_y), see Fig. 6. This orientation is normal to the σ_y trend of the primary stress tensor defined in this region.

We consider that these successive stress states do not represent different tectonic processes related to the margin activity and the interference of the stress field with major structures.

The results are consistent with theoretical models of subduction zones. It is known that decreasing stress magnitudes at the plate margins imply a coaxial change from a reverse regime to strike-slip and normal regimes with no change in the maximum horizontal stress (Tapponier and Molnar 1976; Sassi and Faure 1997). Mechanical compatibility between extensional tensors in intraplate areas and regional compressional and/or strike-slip tensors occurs when σ_y coincides in both ellipsoids. The subducting slab then undergoes different types of stresses at the same time, defining a variety of stress tensors, though all of them are related to the main geodynamic process: subduction and convergence. Four tensors therefore coexist in the study area: a compressional primary stress tensor related to the subduction process and secondaries stress tensors of strike-slip and extensional character, associated with a commensurate reduction in convergence rates and the subduction of the spreading centre below the western margin of the Antarctic Plate. The secondaries stress tensors could be the result of a permutation of the primary stress field.

These permutations and rotations in the principal orientations of the stress axes can only be associated with tectonic processes. Therefore, it is not necessary to explain them in terms of other major geodynamic processes such as complex deformations or stresses transmitted from other active tectonic boundaries, as has been done in the past (*e.g.* Muñoz-Martín *et al.* 1998; Bergerat and Angelier 2000).

The permutations of the axes always originate at changes of location between the principal axes of the stress tensors. Thus, the shape of the stress ellipsoids vary but the axis orientations remain constant (Fig. 6). The more common axis permutations is those in which σ_2 (the intermediate stress axis) interchange its location with σ_1 or σ_3 (the maximum and minimum stress axes, respectively), see Angelier and Bergerat (1983).

With the orientations of the principal stress axes and the stress ratio obtained from fault population analysis, it is also possible to deduce the temporal evolution of the stress field. Subduction with approximately an E-W to NW-SE direction along the NE-SW-trending western margin of the Antarctic Peninsula appears to have been continuous from the Late Triassic (Pankhurst 1982) to the Cenozoic, when the subduction ceased progressively northward. During the early Tertiary, the spreading rates on the Antarctic-Phoenix ridge were about 50 mm/yr, but at 53 Ma (anomaly 24) they decreased to 16–20 mm/yr (Moyes *et al.* 1994). At this moment the stress intensity increased and then the permutations between the stress axes σ_2 and σ_3 could occur, although the stress ellipsoids remained in the same orientation. A change of stress regime took place, from a reverse regime to a wrench regime. The continuous dramatic decrease in the stress once more caused the permutation between the stress axes σ_1 and σ_2. The stress

regime became extensional with a NE-SW direction of σ_3 that could be related to NW-SE-orientated basin development between Alexander Island and Adelaide Island. During the Tertiary, at about 20 to 16.7 Ma, most of the Antarctic-Phoenix ridge sections had collided with the former trench at the Antarctic Peninsula margin (Herron and Tucholke 1976; Barker 1982; Larter and Barker 1991). Subsequent ridge crest-trench collisions caused subduction to cease at 19.8±0.8 Ma off Marguerite Bay, 16.5±0.7 Ma off Adelaide Island and the southern Biscoe Islands, and 14.5±0.6 Ma off the northern Biscoe Islands (Larter and Barker 1991). The subduction of the Antarctic-Phoenix spreading centre below the western margin of Antarctic Plate may have induced the break-up of the forearc, thereby initiating the development of basins on the over-riding plate. The ridge crest-trench subdution induced NW-SE extensional stresses in the overlying plate, bringing about the opening of the George VI trough and George VI Sound with a N trend. This situation did not involve a change in the stress regimen but caused the permutations of the axes σ_2 and σ_3. The proposed model of backarc basin development contrasts with the classical examples in which backarc development in the over-riding plate is induced by the subduction of the leading flank of the spreading centre. The extension in the study area, in contrast, tooks place just shortly after ridge crest-trench collision. Taking into account that subduction may be still active, at least partially, it may be considered as peculiar case of backarc basin. A similar geodynamic evolutionary model has been proposed to explain the development of Jane Basin located in the southeastern part of the South Orkney Microcontinent (Bohoyo *et al.* 2002).

The deformational history of Adelaide Island from brittle mesostructures palaeostress analysis in the southern Wright Peninsula could be correlated with previous work in neighbouring areas. Doubleday and Storey (1998) establish the deformation history of a Mesozoic forearc basin deposits (Fossil Bluff Group) on Alexander Island. This sequence was affected by three phases of deformation: D1 – movement on a major fault in the accretionary complex during the Middle Jurassic with a reverse movement. This fault has been called the LeMay Range Fault and it is located in the eastern edge of Alexander Island. It shows a N-S orientation and dip between 48° to 76° W; D2 – basin inversion in the late Early Cretaceous occurred in a dextral transpressional setting. The mechanisms of inversion of the Fossil Bluff Group have previously been examined by Storey and Nell (1988) and Nell and Storey (1991); and D3 – Cenozoic post-inversion extension that caused the opening of a linear graben, George VI Sound, in a dextral transtensional setting. Edwards (1979) considers that the LeMay Range Fault may represent in this phase the western fault margin of the rift system with a graben which includes the Fossil Bluff Formation of eastern Alexander Island and the George VI Sound. Crabtree *et al.* (1985) suggested that it may have formed at about the same time as ridge crest-trench collisions off Alexander Island in the Early Tertiary. It is interesting to note that the dextral transtensional

movement required to open the trough is consistent with a subduction-dominated regime, as suggested for the LeMay Range Fault implying that extension occurred prior to cessation of subduction. In the same way, Hamilton (1995) suggest that extension has been an important factor in the tectonic development of the Marguerite Bay area, that include the inferred faulted boundaries of the Antarctic Peninsula Batholith, the interpretation of George VI trough as a continuation of George VI Sound, and the predominant NW-SE trends seen in many of the geophysical data sets. Johnson (1997) proposed a two-stage model of the Marguerite Bay area: Stage 1 – a rapid slow-down in plate convergence rates at 52 ma initiates the opening of George VI Sound and George VI trough in a dextral transtension regime; and Stage 2 – the arrival of the Heezen-Tula ridge segment to the south of Adelaide Fracture Zone at 30 Ma stops extension to the south of the Tula Fracture Zone. The extension continues to the north, causing George VI trough to wide, and faulting at the edge of the Antarctic Peninsula Batholith.

Conclusions

The Cenozoic tectonic stress field in the southern Wright Peninsula can be characterized by analysis of brittle mesostructures in Early Paleocene–Eocene rocks. The stress tensors correspond to extensional and compressional regimes. Stress states with a NW-SE trend of σ_1 are compatible with the dominant pattern established for the western Antarctic Peninsula as a result of southeastward progressive subduction of the Phoenix Plate below the Antarctic Plate. The σ_3 orientation shows a relative scattering with two main modes trending NE-SW and NW-SE. Stress states with a NE-SW trend of σ_3 are related to the decreasing relative stress magnitudes from active margins to intraplate regions. On the other hand, stress states with a NW-SE orientation of σ_3 are caused by the develop of a backarc basin related to the subduction of the Antarctic-Phoenix spreading centre below the western margin of the Antarctic Peninsula during the Oligocene–Middle Miocene. This process induced the break-up of the forearc and the beginning of the development of George VI Sound and George VI trough on the over-riding plate.

The successive stress states do not represent different tectonic processes related to the margin activity and the interference of the stress field with major structures. They are due to changes or permutations in principal stress orientations occurring repeatedly in space and time, having been conditioned by the decrease in relative stress magnitudes during the subduction and stretching processes occurring in eastern Adelaide Island, which developed fore-arc or intra-arc basins.

Acknowledgements. — The field work was carried out thanks to the logistic support of the British Antarctic Survey. The authors express their gratitude to the director and the logistic personnel of the British Antarctic Survey, and the *Rothera* station commander. We also acknowledge the very interesting comments of Professor Antoni K. Tokarski, who have improved this paper. This work was supported by the projects CGL2005-03256/ANT and CGL2007-28812E/ANT of the Spanish Ministry of Education and Science.

References

ANGELIER J. and BERGERAT F. 1983. Systèmes de contrainte et extensión intracontinentale. *Bulletin des Centres de Recherches Exploration, Production Elf-Aquitaine* 7: 137–147.

ANGELIER J. and MECHLER P. 1977. Sur une méthode graphique de recherche des contraintres principales également utilisable en tectonique et en séismologie: la méthode des diédres droits. *Bulletin de la Société Géologique de France 7*, 19 (6): 1309–1318.

ARLEGUI L.E. and SIMÓN J.L. 1998. Reliability of palaeostress analysis from fault striations in near multidirectional extension stress fields. Example from the Ebro Basin, Spain. *Journal of Structuctural Geology* 20: 827–840.

ARLEGUI L. and SIMÓN J.L. 2001. Geometry and distribution of regional joint sets in a non-homogeneous stress field: case study in the Ebro basin (Spain). *Journal of Structural Geology* 23: 297–313.

BAHAT D. 1991. *Tectonofractography*. Springer-Verlag, Berlin: 354 pp.

BARKER P.F. 1982. The Cenozoic subduction history of the Pacific margin of the Antarctic Peninsula: Ridge crest-trench interactions. *Journal of the Geological Society, London* 139 (6): 787–801.

BERGERAT F. and ANGELIER J. 2000. The South Iceland Seismic Zone: tectonic and sismotectonic analyses revealing the evolution from rifting to transform motion. *Journal of Geodynamics* 29: 211–231.

BERGERAT F., ANGELIER J. and VERRIER S. 1999. Tectonic stress regimes, rift extension and transform motion: the South Iceland Seismic Zone. *Geodinamica Acta* 12: 303–319.

BERGERAT F., BOUROZ C. and ANGELIER J. 1992. Paleostresses inferred from macrofractures, Colorado Plateau, western U.S.A. *Tectonophysics* 206: 219–243.

BOHOYO F., GALINDO-ZALDÍVAR J., MALDONADO A., SCHRIDER A.A. and SURIÑACH E. 2002. Basin development subsequent to ridge-trench collision: the Jane Basin, Antarctica. *Marine Geophysical Researches* 23: 413–421.

BOTT M.H.P. 1959. The mechanics of oblique slip faulting. *Geological Magazine* 96: 109–117.

CANDE S.C. and KENT D.V. 1995. Revised calibration of the geomagnetic polarity timescale for the Late Cretaceous and Cenozoic. *Journal of Geophysical Research* 100: 6093–6095.

CASAS A.M. and MAESTRO A. 1996. Deflection of a compressional stress field by large-scale basement faults. A case study from the Tertiary Almazán basin (Spain). *Tectonophysics* 255: 135–156.

CASAS A.M., SERÓN F.J. and SIMÓN J.L. 1992. Stress deflection in a tectonic compressional field: a model for the Northwestern Iberian Chain, Spain. *Journal of Geophysical Research* 97: 7183–7192.

CRABTREE R.D., STOREY B.C. and DOAKE C.S.M. 1985. The structural evolution of George VI Sound, Antarctic Peninsula. *Tectonophysics* 114: 431–442.

DE VICENTE G., GINER-ROBLES J.L., MUÑOZ-MARTÍN A., GONZÁLEZ-CASADO J.M. and LINDO R. 1996. Determination of present-day tensor and neotectonic interval in the Spanish Central System and Madrid Basin, central Spain. *Tectonophysics* 266: 405–424.

DOUBLEDAY P.A. and STOREY B.C. 1998. Deformation history of a Mesozoic forearc basin sequence on Alexander Island, Antarctic Peninsula. *Journal of South American Earth Science* 11 (1): 1–21.

EAGLES G. 2003. Tectonic evolution of the Antarctic-Phoenix plate system since 15 Ma. *Earth and Planetary Science Letters* 217: 97–109.

EDWARDS C.W. 1979. New evidence of major faulting on Alexander Island. *British Antarctic Survey Bulletin* 49: 15–20.

ENGELDER T. 1989. Analysis of pinnate joints in the Mount Desert Island granite: Implications for postintrusion kinematics in the coastal volcanic belt, Maine. *Geology* 17: 564–567.

ENGELDER T. and GEISER P. 1980. On the use of regional joint sets as trajectories of paleostress fields during the development of the Appalachian Plateau, New York. *Journal of Geophysical Research* 85 (B11): 6319–6341.

ETCHECOPAR A., VASSEUR G. and DAIGNIERES M. 1981. An inverse problem in microtectonics for the determination of stress tensors from fault population analysis. *Journal of Structural Geology* 3: 51–65.

GARCÍA S., ANGELIER J., BERGERAT F. and HOMBERG C. 2002. Tectonic analysis of the oceanic transform fault zone revealed by fault-slip data and earthquakes focal mechanism: the Housavik-Flately Fault, Iceland. *Tectonophysics* 344: 157–174.

GINER-ROBLES J.L., GONZÁLEZ-CASADO J.M., GUMIEL P. and GARCÍA-CUEVAS C. 2003. Changes in strain trajectories in three different types of plate tectonic boundary deduced from earthquake focal mechanisms. *Tectonophysics* 372: 179–191.

GRIFFITHS C.J. and OGLETHORPE R.D.J. 1998. The stratigraphy and geochronology of Adelaide Island. *Antarctic Science* 10: 462–475.

HAMILTON W.B.1995. Subduction systems and magmatism. *In*: J.L. Smellie (ed.) Volcanism associated with extension at consuming plate margins. *Geological Society Special Publication* 81: 3–28.

HANCOCK P.L. 1985. Brittle microtectonics: Principles and practice. *Journal of Structural Geology* 7: 437–457.

HANCOCK P.L. 1986. Joint Spectra. *In*: I. Nichol and R.W. Nessbit (eds) *Geology in the Real World. The Kingsley Dunham Volume*. Institution of Mining and Metallurgy, London: 155–164.

HANCOCK P.L. and ENGELDER T. 1989. Neotectonic joints. *Bulletin Geological Society of America* 101: 1197–1208.

HARRISON S.M. and PIERCY B.A. 1991. Basement gneisses in north-western Palmer Land: futher evidence for pre-Mesozoic rocks in Lesser Antarctica. *In*: M.R.A. Thomson, J.A. Crame and J.W. Thomson (eds) *Geological evolution of Antarctica*. Cambridge University Press, Cambridge: 341–344.

HERRAIZ M., DE VICENTE G., LINDO-ÑAUPARI R., GINER-ROBLES J.L., SIMÓN J.L., GONZÁLEZ-CASADO J.M., VADILLO O., RODRÍGUEZ-PASCUA M.A., CICUÉNDEZ J.I., CASAS A., CABAÑAS L., RINCÓN P., CORTÉS A.L., RAMÍREZ M. and LUCINI M. 2000. A new perspective about the recent (Upper Miocene to Quaternary) and present tectonic stress distributions in the Iberian Peninsula. *Tectonics* 19: 762–786.

HERRON E.M. and TUCHOLKE B.E. 1976. Sea-floor magnetic patterns and basement structure in the southeastern Pacific. *In*: C.D. Hollister *et al.* (eds) *Initial Reports of the Deep-Sea Drilling Project 35*. US Government Printing Office, Washington, D.C.: 263–278.

HODGSON R.A. 1961. Classification of structures on joint surfaces. *American Journal of Science* 259: 493–502.

JOHNSON A.C. 1997. Cenozoic tectonic evolution of the Marguerite Bay area, Antarctic Peninsula, interpreted from geophysical data. *Antarctic Science* 9 (3): 268–280.

LARTER R.D. and BARKER P.F. 1991. Effects of ridge crest-trench interaction on Antarctic-Phoenix spreading: Forces on a young subducting plate. *Journal of Geophysical Research* 96: 19583–19607.

LARTER R.D., REBESCO M., VANNESTE L.E., GAMBOA P.A.P. and BARKER P.F. 1997. Cenozoic tectonic, sedimentary and glacial history of the continental shelf west of Graham Land, Antarctic Peninsula. *In*: P.F. Barker and A.K. Cooper (eds) Geology and Seismic Stratigraphy of the Antarctic Margin, Part 2. *Antarctic Research Series, American Geophysical Union* 71: 1–27. Washington, D.C.

LEAT P.T. and SCARROW J.H. 1994. Central volcanoes as sources for Antarctic Peninsula Volcanic Group. *Antarctic Science* 6: 365–374.

LEAT P.T., SCARROW J.H. and MILLAR I.L. 1995. On the Antarctic Peninsula batholith. *Geological Magazine* 132: 399–412.

LIVERMORE R., BALANYA J.C., MALDONADO A., MARTINEZ J.M., RODRIGUEZ-FERNANDEZ J., DE GALDEANO C.S., ZALDIVAR J.G., JABALOY A., BARNOLAS A., SOMOZA L., HERNÁNDEZ-MOLINA J., SURIÑACH E. and VISERAS C. 2000. Autopsy on a dead spreading center: The Phoenix Ridge, Drake Passage, Antarctica. *Geology* 28: 607–610.

MILNE A.J. and MILLAR I.L. 1989. The significance of mid-Palaeozoic basement in Graham Land, Antarctic Peninsula. *Journal of the Geological Society, London* 146: 207–210.

MOYES A.B., WILLAN C.F.H., THOMSON J.W. *et al.* 1994. *Geological map of Adelaide Island to Foyn Coast*. BAS GEOMAP Series, Sheet 3, 1:250000, with supplementary text. British Antarctic Survey, Cambridge: 60 pp.

MUÑOZ-MARTÍN A., CLOETINGH S., DE VICENTE G. and ANDEWEG B. 1998. Finite element modelling of Tertiary paleostress fields in the eastern part of the Tajo Basin (central Spain). *Tectonophysics* 300: 47–62.

NELL P.A.R. and STOREY B.C. 1991. Strike-slip tectonics within the Antarctic Peninsula fore-arc. *In*: M.R.A. Thomson, J.A. Crame and J.W Thomson (eds) *Geological evolution of Antarctica*. Cambridge University Press, Cambridge: 443–448.

PANKHURST R.J. 1982. Rb-Sr geochronology of Graham Land, Antarctica. *Journal of the Geological Society, London* 139: 701–711.

PANKHURST R.J., HOLE M.J. and BROOK M. 1988. Isotopic evidence for the origin of Andean granites. *Transactions of the Royal Society of Edinburgh: Earth Sciences* 19: 123–133.

POLLARD D.D. and AYDIN A. 1988. Progress in understanding jointing over the past century. *Geological Society of America Bulletin* 100: 1181–1204.

RIEDEL W. 1929. *Zur mechanik geologischer brucherscheinungen*. Zentralblatt Mineral Geol. Palaeont. Ser. B: 354 pp.

SASSI W. and FAURE J.L. 1997. Role of faults and layer interfaces on the spatial variation of stress regimes in basins: inferences from numerical modelling. *Tectonophysics* 266: 101–119.

SIMÓN J.L. 1986. Análisis of gradual change in stress regime (example from the eastern Iberian Chain, Spain). *Tectonophysics* 124: 37–53.

SIMÓN J.L., ARLEGUI L.E. and POCOVÍ J. 2006. Fringe cracks and plumose structures in layered rocks: stepping senses and their implications for palaeostress interpretation. *Journal of Structural Geology* 28: 1103–1113.

SMITH W.H.F. and SANDWELL D.Y. 1997. Global seafloor topography from satellite altimetry and ship depth sounding. *Science* 277: 1957–1962.

STOREY B.C. and GARRET S.W. 1985. Crustal growth of the Antarctic Peninsula by accretion, magmatism and extension. *Geological Magazine* 122: 5–14.

STOREY B.C. and NELL P.A.R. 1988. Role of strike-slip faulting in the tectonic evolution of the Antarctic Peninsula. *Journal of the Geological Society, London* 145: 333–337.

STRECKEISEN A. 1976. To each plutonic rock its proper name. *Earth Science Reviews* 12: 1–33.

SUÁREZ M. 1976. Plate-tectonic model for southern Antarctic Peninsula and its relation to southern Andes. *Geology* 4: 211–214.

TAPPONIER P. and MOLNAR P. 1976. Slip-line field theory and large-scale continental tectonics. *Nature* 264: 319–324.

THOMSON M.R.A. 1982. Mesozoic paleogeography of West Antarctica. *In*: C. Craddock (ed.) *Antarctic Geoscience*. University of Wisconsin Press, Wisconsin: 331–337.

THOMSON M.R.A. and PANKHURST R.J. 1983. Age of post-Gondwanian calc-alkaline volcanism in the Antarctic Peninsula region. *In*: R.L. Oliver, P.R. James and J.B. Jago (eds) *Antarctic Earth Science*. Australian Academy of Science, Canberra: 328–336.

ZOBACK M.L. 1992. First- and second-order patterns of stress in the lithosphere: the world stress map project. *Journal Geophysical Research* 97: 11703–11728.

Received 17 September 2010
Accepted 22 February 2011